JOURNAL OF VIROLOGY, Aug. 1996, p. 4877–4883 Vol. 70, No. 8
0022-538X/96/$04.00+0

The Concentration of Ca^{2+} That Solubilizes Outer Capsid Proteins from Rotavirus Particles Is Dependent on the Strain

MARIE CHRISTINE RUIZ,[1] ANNIE CHARPILIENNE,[2] FERDINANDO LIPRANDI,[3] RODRIGO GAJARDO,[2] FABIAN MICHELANGELI,[1] AND JEAN COHEN[2]*

Laboratorio de Fisiologia Gastrointestinal[1] and Centro de Microbiologia,[3] Instituto Venezolano de Investigaciones Cientificas, Caracas 1020A, Venezuela, and Laboratoire de Virologie et Immunologie Moléculaires, Institut National de la Recherche Agronomique, Domaine de Vilvert, 78352 Jouy-en-Josas Cedex, France[2]

Received 28 December 1995/Accepted 23 April 1996

It has been previously shown that rotavirus maturation and stability of the outer capsid are calcium-dependent processes. More recently, it has been hypothesized that penetration of the cell membrane is also affected by conformational changes of the capsid induced by Ca^{2+}. In this study, we determined quantitatively the critical concentration of calcium ion that leads to solubilization of the outer capsid proteins VP4 and VP7. Since this critical concentration is below or close to trace levels of Ca^{2+}, we have used buffered solutions based on ethylene glycol-bis(β-aminoethyl ether)-*N*,*N*,*N*′,*N*′-tetraacetic acid (EGTA) and Ca-EGTA. This method allowed us to show a very high variability of the free [Ca^{2+}] needed to stabilize, at room temperature, the outer capsid of several rotavirus strains. This concentration is about 600 nM for the two bovine strains tested (RF and UK), 100 nM for the porcine strain OSU, and only 10 to 20 nM for the simian strain SA11. Titration of viral infectivity after incubation in buffer of defined [Ca^{2+}] confirmed that the loss of infectivity occurs at different [Ca^{2+}] for these three strains. For the bovine strain, the cleavage of VP4 by trypsin has no significant effect on the [Ca^{2+}] that solubilizes outer shell proteins. The outer layer (VP7) of virus-like particles (VLP) made of recombinant proteins VP2, VP6, and VP7 (VLP2/6/7) was also solubilized by lowering the [Ca^{2+}]. The critical concentration of Ca^{2+} needed to solubilize VP7 from VLP2/6/7 made of protein from the bovine strain is close to the concentration needed for the corresponding virus. Genetic analysis of this phenotype in a set of reassortant viruses from two parental strains having the phenotypes of strains OSU (porcine) and UK (bovine) confirmed that this property of viral particles is probably associated with the gene coding for VP7. The analysis of VLP by reverse genetics might allow the identification of the region(s) essential for calcium binding.

Rotavirus capsid has been described as a three-layered structure. The outer layer of complete, highly infectious particles consists of the glycoprotein VP7 and the protein VP4, which is cleaved by proteases into VP5* and VP8*. Proteolysis of triple-layered particles (TLP) increases its ability to infect cultured cells with respect to untrypsinized TLP (UTLP). Double-layered particles (DLP), which lack the outer layer proteins VP4 and VP7 and expose the intermediate protein layer VP6, are not infectious in vitro. The inner layer consists of VP2, which encloses genomic RNA, and the two minor proteins VP1 and VP3. The structure of rotavirus is strongly dependent on the [Ca^{2+}] of the environment. During the replication cycle, from the entry to the release of progeny particles, the forming virion passes through different cellular compartments, each characterized by a distinct [Ca^{2+}] that is determinant for the process. On the basis of in vitro studies with artificial and cell membranes vesicles, it has been hypothesized that penetration of the cell membrane is affected by conformational changes of the capsid induced by Ca^{2+} (24, 27). It has also been suggested that in the infected cell, as occurs in vitro, the low [Ca^{2+}] induces transcriptase activation (5, 20).

After viral RNA and protein synthesis, the final event in the cytoplasmic step of virus morphogenesis is thought to be the budding of DLP into the endoplasmic reticulum (ER) (10, 33), where [Ca^{2+}] reaches the millimolar level. The formation of mature virus is strictly dependent on the concentration of calcium ion present in the growth medium (20, 29). It has been demonstrated that in the absence of Ca^{2+}, VP7 is excluded from hetero-oligomeric complexes, which are normally made of NSP4, VP4, and VP7, and participates in the budding of the DLP into the ER (21, 25). Moreover, calcium depletion of the ER by thapsigargin induced inhibition of VP7 and NSP4 glycosylation as well as virus maturation (23). The cytopathic effect of rotavirus on host cells appears to be mediated by an increase in intracytoplasmic [Ca^{2+}] induced by the synthesis of a viral product (22, 23). NSP4, the transmembrane nonstructural glycoprotein important for viral morphogenesis, affects intracellular calcium homeostasis (34, 35).

It has also been demonstrated that calcium ion has a stabilizing effect on both the virion and VP7; specifically, VP7 synthesized in the presence of calcium was not degraded upon subsequent calcium deprivation (28, 31). Exposing VP7 expressed in a recombinant herpesvirus to a free Ca^{2+} medium [by addition of ethylene glycol-bis(β-aminoethyl ether)-*N*,*N*,*N*′,*N*′-tetraacetic acid (EGTA)] reversibly eliminated neutralizing epitopes, suggesting a calcium-induced conformational change in VP7 (7). Similarly, VP7 synthesized in MA104 cells treated with thapsigargin (which depletes ER of free Ca^{2+}) is not recognized by monoclonal antibodies directed against mature virus VP7 (22). Although sequence conservation among calcium binding sites is not maintained (14), secondary structure analysis and amino acid content suggest that a region of VP7 (amino acids 134 to 146) is a putative calcium binding site (11).

Cryoelectron microscopy and genetic studies clearly demonstrate extensive VP4-VP7 and VP4-VP6 interactions (2, 8, 30, 39). Moreover, an epitope of VP4 has been identified as a

* Corresponding author. Phone: (331) 34 65 26 04. Fax: (331) 34 65 26 21. Electronic mail address: cohen@biotec.jouy.inra.fr.

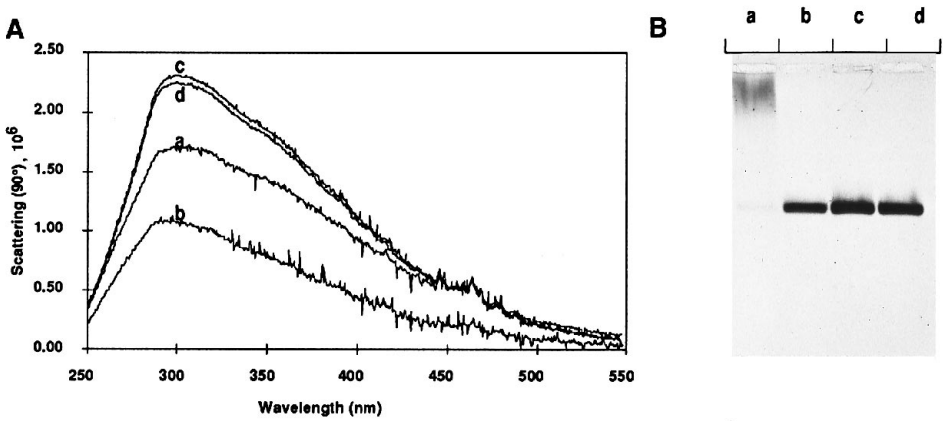

FIG. 1. TLP-to-DLP transition as analyzed by light scattering and gel electrophoresis. Purified TLP (a and b) and DLP (c and d) of the RF strain in 10 mM MOPS–100 mM KCl (pH 7.2) buffer were treated by an excess of EGTA (b and d) or untreated (a and c) and analyzed for changes in perpendicular light scattering spectra (A) and for electrophoretic migration rates in 0.6% agarose gel (B). [EGTA] was 10 mM (A) or 1 mM (B). Scattering units are photometric intensity readings. In panel A, viral proteins concentrations were 5 μg/ml for TLP and 9 μg/ml for DLP. Results of one experiment of a series of three are shown.

critical site for VP4 and VP7 interactions and for virus stability (40).

In this study, we quantitatively determined the critical free [Ca^{2+}] that leads to the solubilization of the outer capsid proteins VP4 and VP7. We also determined the roles of VP4, VP6, and VP7 in the mechanism of outer capsid layer solubilization by low calcium concentrations. It appears that the outer layers of different rotavirus strains are solubilized at very distinct [Ca^{2+}] and that this phenotype is essentially associated with the gene coding for VP7.

MATERIALS AND METHODS

Virus and VLP. Virus strains used in this study (RF, OSU, SA11 4F, SA11 clone 3 [cl3], UK, and RRV) were multiplied in fetal rhesus monkey kidney cells (MA104) after infection at a low multiplicity and in the presence of trypsin (Sigma type IX; 0.44 μg/ml). Strains SA11 4F and SA11 cl3 were kindly provided by M. K. Estes (Baylor College of Medicine, Houston, Tex.). Strain UK was kindly provided by D. Snodgrass (Moredun Research Institute, Edinburgh, Scotland). Strains A131 and A138 were isolated from piglets and are of serotype G3, P9 (OSU-like) (4). Reassortant strains between A131, A138, and UK were produced, and their genomic compositions were characterized as previously described (3). Origins of the genes coding for VP4, VP7, and VP6 were confirmed by serologic analysis using monoclonal antibodies that differentiate the three proteins of the parental strains (3). Virus titration was performed by a plaque assay as described previously (12). To obtain virus with uncleaved VP4, infection was carried out at a high multiplicity and the cell culture medium was supplemented with 1 μg of aprotinin per ml. Virus particles (TLP, UTLP, and DLP) were purified by two runs on a cesium chloride gradient after Freon 113 extraction. Viruslike particles (VLP) were produced by coinfecting Sf9 cells with recombinant baculoviruses at a multiplicity of infection of 5 PFU per cell. The recombinant baculoviruses BacRF2 and BacRF6, containing genes 2 and 6, respectively, of the bovine strain RF, have been described elsewhere (17, 36). The recombinant baculovirus BacRF9Δ, containing the part of gene 9 coding for VP7 but lacking the first signal peptide, was constructed similarly to the recombinant virus containing full-length gene 9 (12). Purification of VLP was performed by two runs in a CsCl gradient in 20 mM piperazine-*N*,*N*′-bis(2-ethanesulfonic acid) (PIPES)–10 μM $CaCl_2$ (pH 6.6) (18 h at 35,000 rpm in a Beckman SW55 Ti rotor). The resulting bands were subjected to zonal centrifugation in a 15 to 45% sucrose gradient in the same buffer (30 min at 40,000 rpm in a Beckman SW55 Ti rotor). In both types of gradient, we consistently observed two bands of VLP, the lower one having VLP with a stoichiometry close to that of the virus particles.

Calcium buffer and virus treatment. Calcium buffers were prepared with CaEGTA and EGTA as described by Tsien and Pozzan (37) in 10 mM morpholinepropanesulfonic acid (MOPS)–100 mM KCl and adjusted to various pHs between 6.6 and 7.8 with concentrated KOH. Calcium concentration was measured with fura-2, using standard calcium calibration buffers from Molecular Probes (Eugene, Oreg.). Purified virus in cesium chloride was desalted and concentrated by pelleting at 100,000 × *g* for 10 min in the TL100:3 rotor of a Beckman TL100 centrifuge. Concentrated stocks of purified virus were alternatively desalted in a Sephadex G-25 column equilibrated with 10 mM MOPS–100 mM KCl adjusted at pH 7.2 with KOH. To study by agarose gel electrophoresis the effect of free [Ca^{2+}] on viral particles, concentrated virus, usually 1 μl, was mixed on ice with a 10-fold-larger volume of Ca^{2+} buffer. Alternatively, we also used 10× Ca^{2+} buffers and mixed 1 volume of virus or VLP with 0.1 volume of 10× buffer. The mixture was then incubated for 10 min at room temperature and loaded on the agarose gel.

Electrophoresis. Electrophoresis of various viral particles or VLP was performed in 0.6% agarose gel in MOPS–10 mM Tris (pH 7.1) buffer. Water used to prepare gels and buffers was produced with a Millipore Milli Q system. Water resistivity was higher than 18 MΩcm, and traces of Ca^{2+} were in the micromolar range as measured with fura-2 and calcium green. Virus (1 volume) incubated in the various conditions was mixed with 1/20 volume of 50% glycerol containing traces of bromophenol blue.

The amount of virus was usually 200 ng per well. In some experiments, loading was performed with the current switched on to ensure a rapid separation of DLP and outer capsid proteins. Electrophoresis was run at room temperature.

Gels were stained either with ethidium bromide (10 μg/ml) or Coomassie blue (0.025% in methanol-acetic acid-water [40:10:50]) or with silver complexes with a Bio-Rad Silver Stain Plus kit. As none of these staining procedures is linear in the range used, it was difficult to define the TLP-to-DLP conversion midpoint. Therefore, we considered only the concentration of Ca^{2+} that leads to 100% conversion to DLP.

Perpendicular light scattering. The TLP-to-DLP transition was monitored by 90° light scattering. For a given concentration of particles, the magnitude of the dispersed light is related to the radius of the particles. We have taken advantage of this property to monitor the transition of TLP to DLP as a change in size. A small volume (5 to 15 μl) of purified virus at the concentration of 900 μg/ml was introduced in the thermostated and stirred cuvette of a spectrofluorimeter (Photon Technology International Inc. model MP1) that contained 1 ml of a Ca^{2+} buffered solution. This solution was prepared as described above and adjusted at pH 7.2 with 10 mM MOPS–100 mM KCl. Slits were adjusted to 0.5 to 1 nm. Scattering wavelength spectrum was obtained by coupled scanning of identical excitation and emission wavelengths. For kinetics experiments, perpendicular scattering was measured by setting both monochromators at a wavelength of 300 nm. Results are presented as relative scattering calculated according to the following equation: relative scattering = $(S_t - S_0)/(S_M - S_0)$, where S_0 is the buffer scattering, S_t is the signal at time t, and S_M is the maximal scattering.

RESULTS

Analysis of the TLP-to-DLP transition by light scattering and electrophoresis. It has been previously shown that chelation of calcium results in the activation of the viral transcriptase and in the solubilization of outer capsid proteins as estimated by differential sedimentation (5). Sedimentation and enzymatic activation do not allow one to easily study the parameters of the TLP-to-DLP transition. In a first series of experiments, we explored the changes of perpendicular light scattering and the rate of migration in an agarose gel of TLP and DLP before and after the addition of EGTA to chelate Ca^{2+}. As shown in Fig. 1A, addition of EGTA to purified TLP (RF strain) resulted in an important change in the light scat-

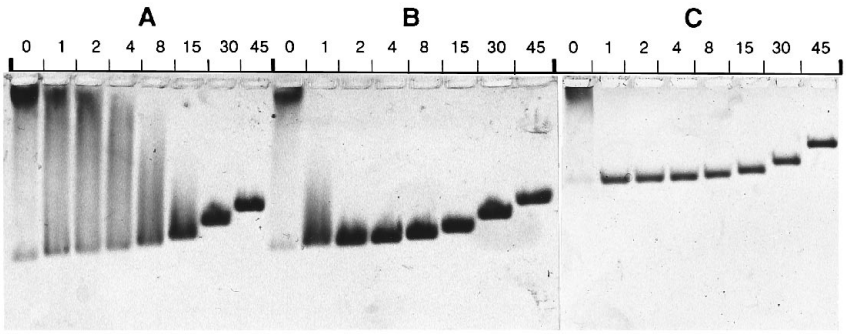

FIG. 2. Kinetics of the TLP-to-DLP transition as analyzed by gel electrophoresis. Purified TLP of the RF strain were incubated at 0°C (A) or at room temperature (B) in 10 mM MOPS–100 mM KCl (pH 7.2) buffered to a free [Ca^{2+}] of 600 nM by 10 mM of EGTA-CaEGTA. Purified TLP rotavirus particles (RF strain) were incubated at 0°C in 1 mM EGTA–10 mM MOPS–100 mM KCl (pH 7.2) (C). At various times (indicated in minutes for each lane), an aliquot was loaded on a 0.6% agarose gel in MOPS-Tris buffer. Electrophoresis started at $t = 0$ and was not interrupted.

tering spectra. The decrease in the intensity of scattered light, relative to the decrease of the radius of particles, is maximal for a wavelength of 300 nm. Addition of EGTA to DLP has no detectable effect on the scattering spectrum. This transition can also be monitored by electrophoresis in 0.6% agarose gels in MOPS-Tris buffer at pH 7.1. This gel system was selected because it minimized the dissociation of the outer capsid proteins from TLP during electrophoresis. In Fig. 1B, it appears that most of the purified TLP of the RF strain migrated as a diffuse band near the entry of the gel. Chelation of Ca^{2+} by 1 mM EGTA resulted in a sharp faster-moving band. These EGTA-treated TLP migrated at the same rate as purified DLP and EGTA-treated DLP. Staining of the nucleic acid moiety of viral particles indicated that both TLP and DLP were permeable to ethidium bromide and that there is no significant decrease in the amount of double-stranded RNA after EGTA treatment (data not shown). These two methods detect changes between TLP and DLP that allow characterization of this transition.

Kinetics of the TLP-to-DLP transition. In a series of preliminary experiments, it was established that the time interval between the treatment of the virus with defined [Ca^{2+}] and electrophoresis was not sufficient for reassociation of outer capsid proteins with DLP to occur (data not shown).

The kinetics of the transition from TLP to DLP was studied at different temperatures and [Ca^{2+}]. Kinetics of the TLP-to-DLP transition could be easily monitored by gel electrophoresis (Fig. 2). At room temperature and a [Ca^{2+}] of 600 nM, the transition was fairly rapid and was complete in less than 2 min (Fig. 2B). At 0°C and the same buffered [Ca^{2+}], the transition was much slower and solubilization of the outer capsid was complete only after 15 min (Fig. 2A). However at 0°C and in Ca^{2+}-free buffer, the reaction was faster and completed in less than 1 min (Fig. 2C). On several lanes in Fig. 2A, a smear appeared between the sharp band of DLP and the broad band of TLP. That band may be the result of a slow solubilization of the outer layer and may correspond to particles that had lost a part of the outer shell proteins.

The changes in particle size under different conditions of [Ca^{2+}] and temperature could be observed in real time by perpendicular light scattering at 300 nm (Fig. 3). At any given [Ca^{2+}], the transition was faster at 37°C than at 20°C. For example, at low [Ca^{2+}] (300 nM), the complete transition occurred in 30 s at 20°C and in less than 8 s at 37°C. At both temperatures, the transition, once initiated, was complete within a time period depending on [Ca^{2+}]. All curves converged at the same minimal scattering value when excess EGTA was added to decrease [Ca^{2+}] to near zero (data not shown).

Concentration of free Ca^{2+} that induces the transition of TLP to DLP. Since the trace concentration of calcium is always above the micromolar range, solubilization of the outer proteins from rotavirus capsid has been studied either at this trace level or at zero Ca^{2+} by addition of EDTA or EGTA in the

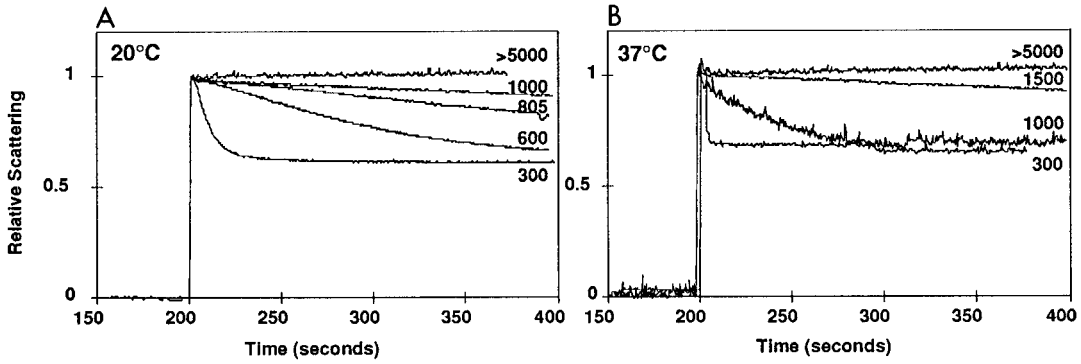

FIG. 3. Kinetics of the TLP-to-DLP transition as analyzed by perpendicular light scattering. Purified TLP of the RF strain (10 μl) were added after 200 s of the onset of recording to a stirred cuvette containing EGTA-CaEGTA buffers adjusted to various [Ca^{2+}] and maintained at 20°C (A) or 37°C (B). Perpendicular light scattering was measured at a wavelength of 300 nm. Results are presented as relative scattering as described in Materials and Methods. Numbers correspond to buffered free Ca^{2+} concentration (nanomolar). Results of one experiment of a series of two are shown.

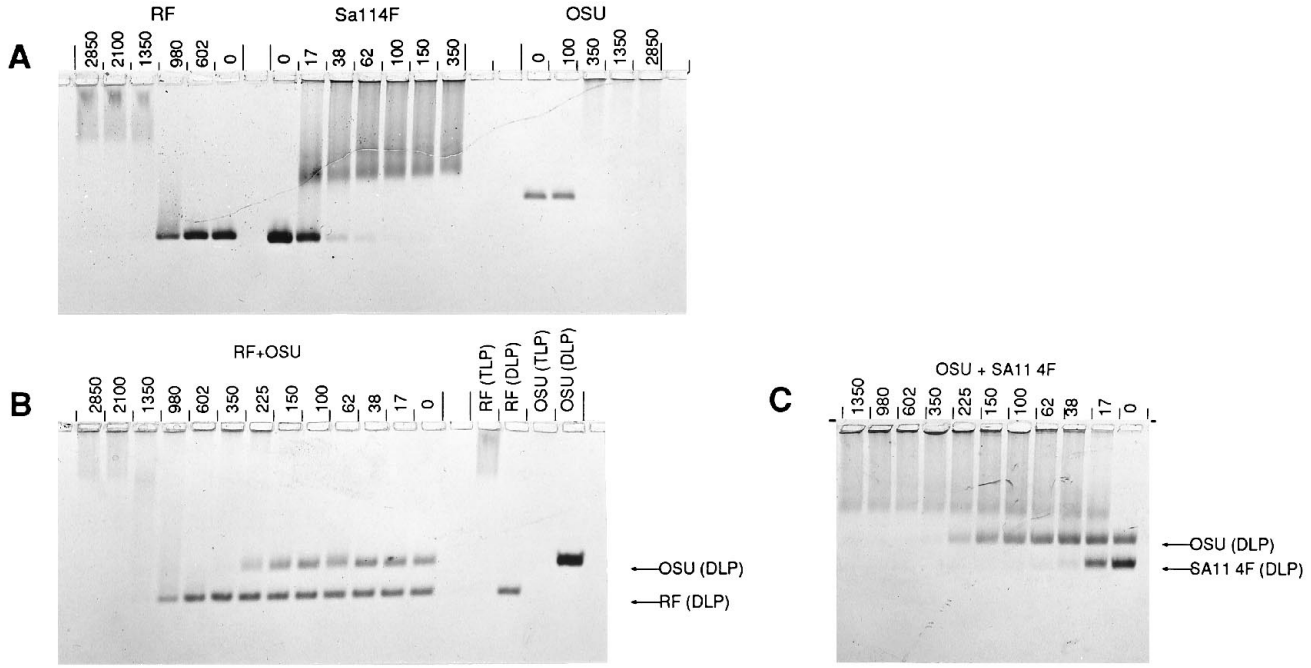

FIG. 4. Sensitivities of various rotavirus strains to [Ca^{2+}]. Purified TLP from strains RF, SA11 4F, and OSU were separately treated with various EGTA-CaEGTA buffers adjusted to various [Ca^{2+}] (nanomolar) as indicated at the top, either separately (A) or as a mixture of RF and OSU (B) or SA11 4F and OSU (C). Adjusted amounts of each strain were mixed and pelleted. The pellets were resuspended in 10 mM MOPS–100 mM KCl (pH 7.2) buffer, and aliquots were added with 10× EGTA-CaEGTA buffers adjusted to the [Ca^{2+}] indicated at the top. After a 10-min treatment at room temperature, samples were loaded on the gel. Unmixed TLP and DLP from strains RF and OSU were included in panel B as controls.

millimolar range. In this work, we explored the stability of the outer capsid, for several rotavirus strains, in the micromolar to nanomolar range by using buffered Ca^{2+} solutions. Purified bovine strain RF was incubated at pH 7.2 for 10 min at room temperature in buffered Ca^{2+} solutions having a [Ca^{2+}] from 5 μM to 10 nM. As shown in Fig. 4A, there is a transition for a [Ca^{2+}] of about 1,000 nM, and the complete conversion into DLP occurs at 600 nM. As observed in kinetics analysis (Fig. 2A), it appeared that at the critical concentration (e.g., 980 nM for the RF strain), part of the particles migrated between DLP and TLP. The same experiments were performed with the porcine strain OSU and the simian strain SA11 4F. All of the genes in the latter strain are of simian origin except the gene coding for VP4, which is of bovine origin. For strains OSU and SA11 4F, the transition of TLP to DLP began at about 200 and 20 nM, respectively. The complete conversion was observed at 100 nM for OSU and 0 nM for SA11 4F. DLP of strains RF and SA11 4F migrated at the same rate in this gel system, but surprisingly, OSU DLP migrated more slowly (Fig. 4A). This difference allowed us to compare pairs of strains treated simultaneously with various Ca^{2+} buffers, thus excluding the possibility that the difference between strains was due to variations during treatment with low calcium or during electrophoresis. As shown in Fig. 4, we compared RF and OSU (Fig. 4B) and then SA11 4F and OSU (Fig. 4C). In all cases, we found the same values of [Ca^{2+}] for the transition and the same differences between strains as shown in Fig. 4A. This comparison was extended to other strains. We have determined that strains RRV and SA11 cl3 have the same stability relative to [Ca^{2+}] as strain SA11 4F. The porcine strains A131 and A138 have the same stability as strain OSU, and strain RF has the same stability as the bovine strain UK (data not shown).

Since solubilization of the outer layer induces a loss of infectivity, we confirmed the different sensitivities of the strains RF, OSU, and SA11 4F by titrating virus stocks after treatment for 10 min in a solution buffered at a [Ca^{2+}] of 100 nM. In these conditions, the RF strain titer decreased from 3×10^8 to 7×10^2 PFU/ml and the OSU strain titer decreased from 10^8 to 10^4 PFU/ml. As expected, strains SA11 4F and SA11 cl3 showed no significant titer decrease after treatment by 100 nM of Ca^{2+}.

Effect of pH on solubilization by low [Ca^{2+}]. All of the experiments described above were performed at pH 7.2. Next, we examined whether solubilization by low calcium could also be dependent on pH. Since the K_D of EGTA for Ca^{2+} changes fairly rapidly with pH, it is critical to study the effects of pH changes in a range of [Ca^{2+}] at which EGTA-CaEGTA has a good buffering capacity. For this reason, we tested the OSU strain, whose transition occurs at 200 nM. As shown in Fig. 5, pH changes in the range of 6.8 to 7.6 had no significant effect on the concentration of Ca^{2+} that solubilizes the outer layer proteins.

VP7 has a major role in the differential stability to low [Ca^{2+}]. Reassortant viruses prepared from two parental viruses having different phenotypes were used to map the gene responsible for stability of the capsid in low [Ca^{2+}]. As shown in Table 1, the parental strain UK, of bovine origin, needs a [Ca^{2+}] of 600 nM for complete solubilization of outer protein layer, whereas the two porcine parental strains, A131 and A138, need 100 to 150 nM. All of the reassortants expressing a porcine VP7 from A138 or A131 lost their outer capsids at a [Ca^{2+}] of about 100 nM (50 to 150 nM), regardless the origin of either VP4 or VP6. In contrast, reassortant TO7, with a VP7 from the UK parent, required 500 nM [Ca^{2+}] for the solubilization of its external capsid, although it bears a porcine VP4.

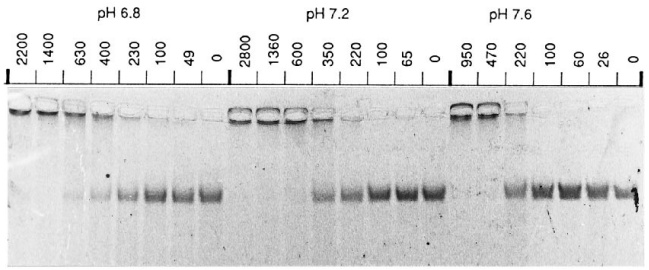

FIG. 5. Effect of pH on the minimal [Ca^{2+}] needed to induce the TLP-to-DLP transition. Purified TLP from strain OSU were treated in various EGTA-CaEGTA buffers at different pHs for 10 min before being electrophoresed in 0.6% agarose gels as previously described. The changes of affinity of EGTA for Ca^{2+} depending on the pH was taken into account, and calculated concentrations of Ca^{2+} (nanomolar) are indicated above the lanes.

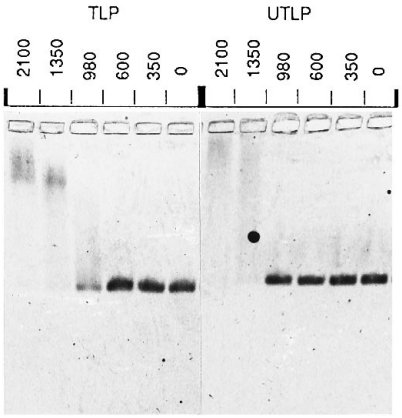

FIG. 6. Effect of low [Ca^{2+}] on TLP and UTLP. Purified UTLP and TLP from the RF strain of rotavirus were treated for 10 min at room temperature in 10 mM MOPS–100 mM KCl (pH 7.2) with the buffered concentration (nanomolar) of Ca^{2+} indicated on the top, loaded on a 0.6% agarose gel, and electrophoresed.

These results suggest that the nature of VP7 determines the stability of the outer capsid. Genes coding for VP6 and VP4 have no major effect on the stability at low [Ca^{2+}] in this gene constellation. Since it has been shown that the two proteins of the outer layer interact, we also looked for an effect of the trypsin cleavage of VP4 on the [Ca^{2+}] that solubilizes the outer layer. As shown in Fig. 6, trypsinization had no significant effect on the concentration of Ca^{2+} needed to solubilize the outer capsid layer.

VLP and authentic virions are similarly affected by low [Ca^{2+}]. Coexpression of capsid proteins VP2 and VP6 in the baculovirus-insect cell system results in VLP having a morphology similar to that of DLP and referred to as VLP2/6 (6, 17). Similarly, the coexpression of VP2, VP6, and VP7 results in particles (referred to as VLP2/6/7) having, in negative staining, the morphology of complete virions. By electrophoresis in agarose gel, VLP2/6 migrated faster and in a more diffuse manner than their authentic viral counterparts, the DLP (Fig. 7). The addition of minor proteins VP1 and VP3, which assemble in VLP when coexpressed with VP2 and VP6, did not change band sharpness (data not shown). This finding indicated that VLP are less homogeneous, in size and/or in charge, than virus particles. As with the comparison of the OSU strain with the other strains, we took advantage of the different rates of migration of DLP from RF and VLP2/6 to study in the same gel lane the [Ca^{2+}] that solubilize the outer layer. Purified TLP and VLP2/6/7 were mixed and simultaneously incubated with Ca^{2+} buffered solutions. As shown in Fig. 7, VLP2/6/7, consisting of proteins derived from the bovine strain RF, had the VP7 outer layer solubilized when the concentration of Ca^{2+} was below 1,000 nM. This value is slightly higher than the value found for the virus (RF strain) and indicated that VP4 might have a minor role in the calcium-dependent transition from TLP to DLP.

TABLE 1. [Ca^{2+}] needed for solubilization of the outer protein layer[a]

Reassortant	Origin of:			[Ca^{2+}] (nM)
	VP4	VP6	VP7	
A131				150
A138				110
UK				600
TO7	A138	UK	UK	500
T15	UK	UK	A138	50
VV21	A131	UK	A131	100
VV38	UK	UK	A131	100
VV25	UK	A131	A131	150

[a] Reassortants derived from the UK bovine strain of rotavirus and two porcine strains (A131 and A138) were analyzed for the [Ca^{2+}] inducing the TLP-to-DLP transition. Indicated values are averages of at least two determinations and correspond to a complete conversion to DLP.

DISCUSSION

For several animal and plant viruses, it has been shown that calcium ion, as well as H^+, plays a role in the capsid assembly, stability, and disassembly (1, 9). Moreover, it has been shown that various strains of the same virus can be more or less sensitive to H^+ concentration (32). To our knowledge, this is the first report showing that very different calcium concentrations are required to stabilize various strains of the same virus. These differences between strains contrast with the fact that no

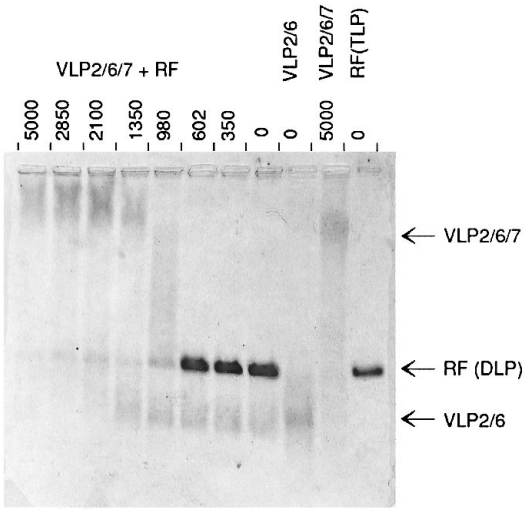

FIG. 7. Comparison of solubilization of outer protein(s) from virus and VLP obtained in the baculovirus system. Purified VLP made in the baculovirus system by coexpression of VP2, VP6, and VP7 from the RF strain were mixed with purified TLP from the RF strain. The mixture was incubated in a series of EGTA-CaEGTA buffers having the [Ca^{2+}] (nanomolar) indicated at the top. VLP 2/6/7 in the absence or presence of Ca^{2+} (1 mM EGTA or 10 μM $CaCl_2$, respectively) and TLP of rotavirus are presented on the right as controls.

remarkable differences in acid resistance between different rotavirus strains have been detected (38). Our results indicate that the Ca^{2+}-dependent stability of rotavirus is essentially related to the gene coding for the outer glycoprotein VP7. The use of calcium buffered solutions allowed us to precisely define the critical concentration that solubilized the outer layer. Analysis of this process by light scattering and by gel electrophoresis indicated that the kinetics of solubilization is dependent on the temperature and the concentration of free Ca^{2+}. At a concentration of 300 nM, which is higher than the average intracytoplasmic [Ca^{2+}], complete solubilization of the outer layer of the RF strain is obtained in less than 8 s at 37°C. Kinetics at low temperature or at the critical concentration of free Ca^{2+} resulted in a smear upon electrophoresis, indicating that in these conditions, it is possible to obtain particles with the outer layer partially removed. As suggested by the relatively low decrease of OSU titer after 100 nM Ca^{2+} treatment, these particles having a part of their outer layer are probably infectious.

It has been previously indicated that agarose gel electrophoresis separates various kinds of rotavirus particles, like various kinds of macromolecular assembly, according to their sizes (13, 16, 18). The diffuse band observed with TLP suggested that purified viruses may not carry the full complement of 60 spikes (120 molecules) of VP4 or have an heterogeneity of the stoichiometry of VP7. Similarly, the broad band of VLP2/6, which contrasts with the sharp band of DLP, could reflect the heterogeneity of VP6 assembly on corelike particles made of VP2. Moreover, our results showed clearly that migration of TLP and DLP is also affected by other parameters, most probably by the charge of particles. In this respect, we found that according to the virus strain, TLP migrated differently, or even did not enter the gel, at the pH used (e.g., Fig. 4, strain OSU). Similarly, the migration of DLP from OSU (and the two other porcine strains tested) is significantly slower than the migration of the bovine and simian strains tested, even though it could be assumed that the radii of DLP from various strains are identical. Analysis of the reassortant viruses indicated that this phenotype of DLP could be related to VP6 (not shown). However, the nucleic acid moiety of particle could also play a role in the rate of migration. Further studies with VLP made of proteins from various viral origins are needed to clarify this point.

Analysis of the phenotypes of reassortant viruses suggests that VP7 is probably the protein implicated in the interaction between calcium and viral particle. However it cannot be excluded that VP1, VP2, and VP3 (and eventually the genomic RNA itself) are also implicated, since the genotypes of the reassortant viruses used have not been fully characterized because of comigration of parental segments 1, 2, and 3. Three observations indicated that VP4 plays a minor role in the calcium-dependent solubilization of the outer capsid, and this may be through its well-established interactions with VP7: (i) the Ca^{2+}-dependent stability of VP7 in VLP devoid of VP4 is similar to that of VP7 in virus particles; (ii) SA11 cl3 and SA11 4F are equally resistant to low [Ca^{2+}] even though they differ only in gene 4, which is of bovine origin for SA11 4F; and (iii) cleavage of VP4 by trypsin did not significantly change the [Ca^{2+}] needed to solubilize the outer layer.

The major role of VP7 in the phenotype described here is consistent with previously published data showing that the conformation and stability of VP7 are Ca^{2+} dependent (7, 28). It may be possible that the calcium binding site is entirely within a single molecule of VP7 and that the conformation change due to the absence of the ion in that site induces indirectly a break of intermolecular binding. Since it has been recently shown that Ca^{2+} can directly mediate protein-protein interactions (26), it could be alternatively hypothesized that calcium ion plays a direct role in the cohesion of the outer layer, creating a physical link either between VP7 trimers or between VP7 monomers. In another system, the viral capsid of simian virus 40, Ca^{2+} forms a bridge between a C-terminal arm of one pentamere and an internal loop of another one (19). In this case, Ca^{2+} binding by VP7 in intact rotavirus particles would be probably of a cooperative nature, with ligands for calcium binding contributed by domains from more than one VP7 molecule.

The biological significance of differences between strains with respect to the calcium concentration that solubilizes the outer layer is not clear. The intracytoplasmic concentration of calcium has been measured in various cells, and the average value for resting cell is between 100 and 20 nM (15, 23). The dissociation of the outer capsid, which triggers the structural transcriptase, occurs at a concentration that is, for the strains tested, higher than (or equal to, for SA11) the average cytoplasmic [Ca^{2+}]. Thus, our observations are consistent with the hypothesis (5, 20) that transcriptase is activated after virus penetration into the cell upon encountering a low-Ca^{2+} environment such as in the cytoplasm. The use of site-directed mutations in VLP, as well as the selection of mutants that are resistant to low concentrations of calcium, may allow the identification of the regions of VP7 essential for calcium binding. Both strategies are now being explored.

ACKNOWLEDGMENTS

We are very grateful to Max Ciarlet, who provided the reassortant rotaviruses.

R. Gajardo is funded in part by a fellowship from Formacion de Personal Investigador en el Extranjero del Ministerio de Educacion y Cienca de España. This work was supported in part the France-Venezuela cooperation program and by CONICIT (Venezuela) grant MPS-RP-IV-140031.

REFERENCES

1. **Brady, J. N., V. D. Winston, and R. A. Consigli.** 1977. Dissociation of polyoma virus by the chelation of calcium ions found associated with purified virions. J. Virol. **23:**717–724.
2. **Chen, D. Y., M. K. Estes, and R. F. Ramig.** 1992. Specific interactions between rotavirus outer capsid proteins VP4 and VP7 determine expression of a cross-reactive, neutralizing VP4-specific epitope. J. Virol. **66:**432–439.
3. **Ciarlet, M., M. Hidalgo, and F. Liprandi.** 1996. Cross-reactive, serotype- and monotype-specific neutralization epitopes on VP7 of serotype G3 and G5 porcine rotavirus strains. Arch. Virol. **141:**601–604.
4. **Ciarlet, M., J. E. Ludert, and F. Liprandi.** 1995. Comparative amino acid sequence analysis of the major outer capsid protein (VP7) of porcine rotaviruses with G3 and G5 serotype specificities isolated in Venezuela and Argentina. Arch. Virol. **140:**437–451.
5. **Cohen, J., J. Laporte, A. Charpilienne, and R. Scherrer.** 1979. Activation of rotavirus RNA polymerase by calcium chelation. Arch. Virol. **60:**177–186.
6. **Crawford, S. E., M. Labbé, J. Cohen, M. H. Burroughs, Y. J. Zhou, and M. K. Estes.** 1994. Characterization of virus-like particles produced by the expression of rotavirus capsid proteins in insect cells. J. Virol. **68:**5945–5952.
7. **Dormitzer, P. R., and H. B. Greenberg.** 1992. Calcium chelation induces a conformational change in recombinant herpes simplex virus-1-expressed rotavirus VP7. Virology **189:**828–832.
8. **Dormitzer, P. R., D. Y. Ho, E. R. Mackow, E. S. Mocarski, and H. B. Greenberg.** 1992. Neutralizing epitopes on herpes simplex virus-1-expressed rotavirus VP7 are dependent on coexpression of other rotavirus proteins. Virology **187:**18–32.
9. **Durham, A. C. H., D. A. Hendry, and M. B. von Wechmar.** 1977. Does calcium ion binding control plant virus disassembly? Virology **77:**524–533.
10. **Estes, M. K.** 1990. Rotaviruses and their replication, p. 1324–1352. *In* B. Fields and D. M. Knipe (ed.), Virology. Raven Press, New York.
11. **Estes, M. K., and J. Cohen.** 1989. Rotavirus gene structure and function. Microbiol. Rev. **53:**410–449.
12. **Franco, M. A., I. Prieto, M. Labbé, D. Poncet, C. F. Borras, and J. Cohen.** 1993. An immunodominant cytotoxic T cell epitope on the VP7 rotavirus protein overlaps the H2 signal peptide. J. Gen. Virol. **74:**2579–2586.
13. **Gallegos, C. O., and J. T. Patton.** 1989. Characterization of rotavirus repli-

cation intermediates: a model for the assembly of single-shelled particles. Virology **172:**616–627.
14. **Haiech, J., and J. Sallantin.** 1985. Computer search of calcium binding sites in a gene data bank: use of learning techniques to build an expert system. Biochimie **67:**555–560.
15. **Irurzun, A., J. Arroyo, A. Alvarez, and L. Carrasco.** 1995. Enhanced intracellular calcium concentration during poliovirus infection. J. Virol. **69:**5142–5146.
16. **Konarska, M. M., and P. A. Sharp.** 1987. Interactions between small nuclear ribonucleoprotein particles in formation of spliceosomes. Cell **49:**763–774.
17. **Labbé, M., A. Charpilienne, S. E. Crawford, M. K. Estes, and J. Cohen.** 1991. Expression of rotavirus VP2 produces empty corelike particles. J. Virol. **65:**2946–2952.
18. **Larson, S. M., J. B. Antczak, and W. K. Joklik.** 1994. Reovirus exists in the form of 13 particle species that differ in their content of protein sigma 1. Virology **201:**303–311.
19. **Liddington, R. C., Y. Yan, J. Moulai, T. L. Benjamin, and S. C. Harrison.** 1991. Structure of simian virus 40 at 3.8-Å resolution. Nature (London) **354:**278–284.
20. **Ludert, J. E., F. Michelangeli, F. Gil, F. Liprandi, and J. Esparza.** 1987. Penetration and uncoating of rotaviruses in cultured cells. Intervirology **27:**95–101.
21. **Maass, D. R., and P. H. Atkinson.** 1990. Rotavirus proteins VP7, NS28, and VP4 form oligomeric structures. J. Virol. **64:**2632–2641.
22. **Michelangeli, F., F. Liprandi, M. E. Chemello, M. Ciarlet, and M. C. Ruiz.** 1995. Selective depletion of stored calcium by thapsigargin blocks rotavirus maturation but not the cytopathic effect. J. Virol. **69:**3838–3847.
23. **Michelangeli, F., M.-C. Ruiz, J. Castillo, J. Ludert, and F. Liprandi.** 1991. Effect of rotavirus on intracellular calcium homeostasis in cultures cells. Virology **181:**520–527.
24. **Nandi, P., A. Charpilienne, and J. Cohen.** 1992. Interaction of rotavirus particles with liposomes. J. Virol. **66:**3363–3367.
25. **Poruchynsky, M. S., D. R. Maas, and P. H. Atkinson.** 1991. Calcium depletion blocks the maturation of rotavirus by altering the oligomerization of virus-encoded proteins in the ER. J. Cell Biol. **114:**651–661.
26. **Rao, Z., P. Handford, M. Mayhew, V. Knott, G. G. Brownlee, and D. Stuart.** 1995. The structure of a Ca^{2+} epidermal growth factor-like domain: its role in protein-protein interactions. Cell **82:**131–141.
27. **Ruiz, M. C., T. S. Alonso, A. Charpilienne, M. Vasseur, F. Michelangeli, J. Cohen, and F. Alvarado.** 1994. Rotavirus interaction with isolated membrane vesicles. J. Virol. **68:**4009–4016.
28. **Shahrabadi, M. S., L. A. Babiuk, and P. W. K. Lee.** 1987. Further analysis of the role of calcium in rotavirus morphogenesis. Virology **158:**103–111.
29. **Shahrabadi, M. S., and P. W. K. Lee.** 1986. Bovine rotavirus maturation is a calcium-dependent process. Virology **152:**298–307.
30. **Shaw, A. L., R. Rothnagel, D. Chen, R. F. Ramig, W. Chiu, and B. V. Prasad.** 1993. Three-dimensional visualization of the rotavirus hemagglutinin structure. Cell **74:**693–701.
31. **Shirley, J. A., G. M. Beards, M. E. Thouless, and T. H. Flewett.** 1981. The influence of divalent cations on the stability of human rotavirus. Arch. Virol. **67:**1–9.
32. **Skern, T. H. T., H. Auer, E. Kuechler, and D. Blaas.** 1991. Human rhinovirus mutants resistant to low pH. Virology **183:**757–763.
33. **Suzuki, H., T. Konno, and Y. Numazaki.** 1993. Electron microscopic evidence for budding process-independent assembly of double-shelled rotavirus particles during passage through endoplasmic reticulum membranes. J. Gen. Virol. **9:**2015–2018.
34. **Tian, P., M. K. Estes, Y. F. Hu, J. M. Ball, C. Q. Y. Zeng, and W. P. Schilling.** 1995. The rotavirus nonstructural glycoprotein NSP4 mobilizes Ca^{2+} from the endoplasmic reticulum. J. Virol. **69:**5763–5772.
35. **Tian, P., Y. Hu, W. P. Schilling, D. A. Lindsay, J. Eiden, and M. K. Estes.** 1994. The nonstructural glycoprotein of rotavirus affects intracellular calcium levels. J. Virol. **68:**251–257.
36. **Tosser, G., M. Labbé, M. Brémont, and J. Cohen.** 1992. Expression of the major capsid protein VP6 of group C rotavirus and synthesis of chimeric single-shelled particles by using recombinant baculoviruses. J. Virol. **66:**5825–5831.
37. **Tsien, R., and T. Pozzan.** 1989. Measurement of cytosolic free Ca^{2+} with Quin 2. Methods Enzymol. **172:**230–263.
38. **Weiss, C., and H. F. Clark.** 1985. Rapid inactivation of rotaviruses by exposure to acid buffer or acidic gastric juice. J. Gen. Virol. **66:**2725–2730.
39. **Yeager, M., J. A. Berriman, T. S. Baker, and A. R. Bellamy.** 1994. Three-dimensional structure of the rotavirus haemagglutinin VP4 by cryo-electron microscopy and difference map analysis. EMBO J. **13:**1011–1018.
40. **Zhou, Y. J., J. W. Burns, Y. Morita, T. Tanaka, and M. K. Estes.** 1994. Localization of rotavirus VP4 neutralization epitopes involved in antibody-induced conformational changes of virus structure. J. Virol. **68:**3955–3964.